

GaAs Microwave power HBTs for Mobile Communications

M. Achouche, S. Kraus, T. Spitzbart, S. Hähle, W. John, M. Mai, D. Rentner, P. Wolter, H. Wittrich, T. Bergunde, F. Brunner, P. Kurpas, E. Richter, M. Weyers, J. Würfl, G. Tränkle

Ferdinand-Braun-Institut für Höchstfrequenztechnik (FBH)

Albert Einstein Straße, 11

12489 Berlin, Germany

E-mail: achouche@fbh-berlin.de

Abstract: A 1 W output power (2.8 W/mm) GaAs-based HBT with more than 56 % power added efficiency at 3 V operating bias for use in mobile communications is described. Device layout and technology are optimized to obtain high microwave performance with low thermal resistance and compact chip size. The fabricated sub-cell power HBTs with $3 \times 30 \mu\text{m}^2$ emitter area yield a maximum current gain of 90 with $f_{\text{max}} > 100$ GHz. The power cell HBT, which has $12 \times 3 \times 30 \mu\text{m}^2$ emitter area exhibits 3 W (8.4 W/mm) output power and 70 % power added efficiency at $V_{\text{CE}}=8$ V while maintaining high performance at low supply bias of 3 V.

I. INTRODUCTION

GaAs-HBTs have been widely accepted in many RF-microwave applications including power amplifiers, oscillators and mixers. For the mobile telephone market which is considered to be the major driver in establishing a profitable GaAs technology, power amplifiers based on GaAs-HBTs can offer remarkable microwave power capabilities and efficiency. Actually, the currently available power amplifiers for PCN applications are based on GaAs-MESFETs. This technology offers good performance but still suffers from low power density resulting in large chip sizes to meet the requirement for output power above 30 dBm. As an alternative, GaAs HBTs and enhancement mode PHEMTs are considered excellent candidates for use as power devices due to their ability to operate with single supply voltage.

In this work, AlGaAs/GaAs and InGaP/GaAs HBTs are developed using production-like processes (i-line stepper, 3" and 4" wafers) for microwave power application. The fabricated power cell HBTs with $1080 \mu\text{m}^2$ emitter area yield a small signal gain MUG and MAG @ 2 GHz of 31 dB and 24 dB, respectively. Using this technology,

$12 \times 3 \times 30 \mu\text{m}^2$ power cell HBTs exhibit 1 W output power and more than 56% power added efficiency at 3 V operating bias.

II. DEVICE PROCESSING

The In-house MOCVD-grown HBT layer structure mainly consists of a 65 nm N-AlGaAs graded emitter layer ($N=3 \times 10^{17} \text{cm}^{-3}$) (or a 30 nm N-InGaP for InGaP HBTs), an 100 nm p-GaAs uniformly doped base layer ($p=4 \times 10^{19} \text{cm}^{-3}$), a 1000 nm-thick n-GaAs ($n=2 \times 10^{16} \text{cm}^{-3}$) collector layer, and a 700 nm-thick ($n=5 \times 10^{18} \text{cm}^{-3}$) n-GaAs subcollector layer. Dopants are Si and C for n-type and p-type layers, respectively.

The power HBT process uses a double-mesa approach to access the base and collector. Device isolation is ensured by He^+ ion implantation. The process flow of our L-band HBTs fabrication has been already reported and is mainly based on a selective dry-etching process for emitter mesa realization [1]. The emitter, base and collector electrodes consist of WSiN/Ti/Pt/Au, Pt/Ti/Pt/Au and Ni/Ge/Au/Ni/Au metal systems, respectively. Emitter finger interconnection is made by Ti/Pt/Au metal evaporation or/and 10 μm or 20 μm electroplated gold (thermal shunt). Fig.1 shows an SEM picture of an L-Band sub-cell HBT.

The wafer average DC current gain is 90 with a dispersion of 8 % (this value has been obtained on two different batches of $5 \times 3''$). The intrinsic base sheet resistance is $200 \Omega/\square$ with a dispersion of 7 % over the wafer.

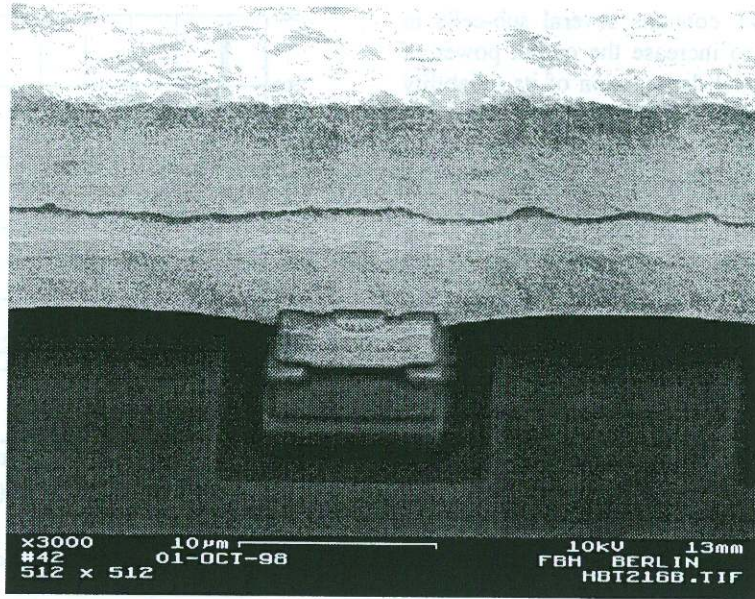


Fig. 1 L-Band power sub-cell HBT with 20 μm thermal shunt technology

III. DEVICE PERFORMANCE

Typical I-V curves for an AlGaAs-GaAs HBT with an emitter size of $3 \times 30 \mu\text{m}^2$ (sub-cell) are shown in Fig. 2-a. The power HBT reaches a $1 \times 10^5 \text{ A/cm}^2$ collector current density level at a V_{CE} of 0.6 V, indicating a good collector turn-on characteristic and shows a low off-set voltage of about 0.1 V. All these characteristics are favorable for high efficient devices operating at low bias supply voltage. The collector-base breakdown voltage BV_{CBO} is 22 V. Fig. 2-b shows RF characteristics of a $3 \times 30 \mu\text{m}^2$ area HBT (AlGaAs/GaAs) at a collector current density of $J_{\text{CE}} = 3 \times 10^4 \text{ A/cm}^2$. An f_t of 31 GHz and an f_{max} of 105 GHz are extrapolated. The average f_t is 32 GHz with an f_{max} of 101 GHz. Standard deviations are 2 GHz and 6 GHz, respectively. The small signal gain MUG @ 2 GHz and MAG @ 2 GHz are 33 dB and 26 dB, respectively. Small signal gain MAG remains high even at 10 GHz (18.5 dB).

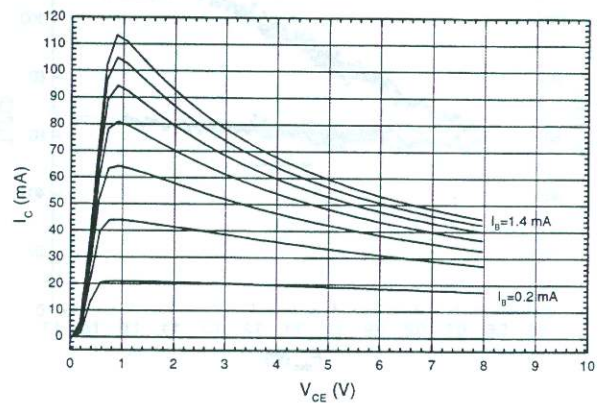


Fig. 2-a $I_{\text{CE}}-V_{\text{CE}}$ characteristics of an AlGaAs/GaAs-HBT ($3 \times 30 \mu\text{m}^2$)

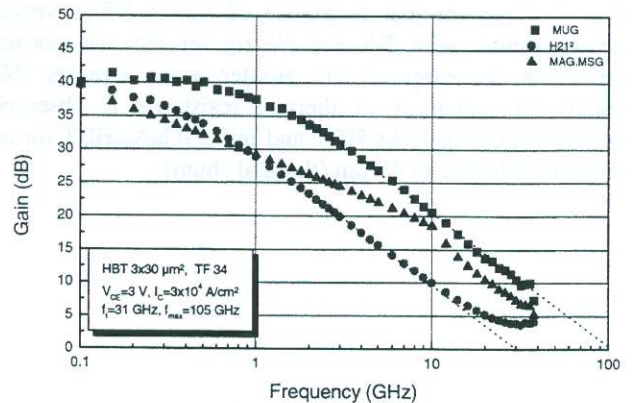


Fig. 2-b RF characteristics of a $3 \times 30 \mu\text{m}^2$ AlGaAs-GaAs-HBT ($J_{\text{CE}} = 3 \times 10^4 \text{ A/cm}^2$)

A typical power cell HBT contains several sub-cells in parallel. The objective is to increase the output power of the device without substantial degradation of its reliability and microwave performance. Using a thermal shunt technology, power cell HBTs with $12 \times 30 \mu\text{m}^2$ emitter area have a small signal gain MUG @ 2 GHz and MAG @ 2 GHz of 31 dB and 24 dB, respectively, which constitute a degradation of only 2 dB compared to the sub-cell. In addition, to manage the heat generated during power operation, it is important to improve device thermal dissipation by reducing device thermal resistance and thus its junction temperature. Fig. 3 shows as an example the variations of thermal resistance R_{th} and junction temperature T_j against dissipated power P_{diss} for a power cell HBT. Thermal resistance measurements requires only the measurement of the HBT DC output characteristics at two different temperatures as described in Reference [2].

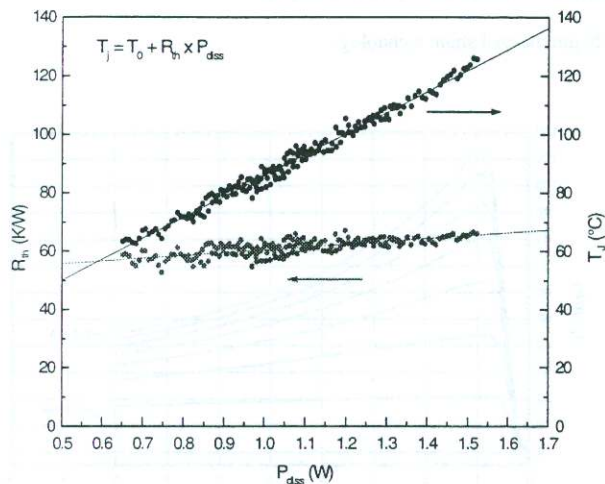


Fig. 3 Thermal resistance R_{th} and junction temperature T_j versus dissipated power P_{diss}

Fig. 4 shows thermal resistance of power HBTs versus device emitter area. We can clearly see that the thermal resistance decreases as the emitter area increases. No significant variations of thermal resistance is observed between AlGaAs/GaAs-HBT and InGaP/GaAs-HBT for an emitter air-bridge of $10 \mu\text{m}$ (thermal shunt).

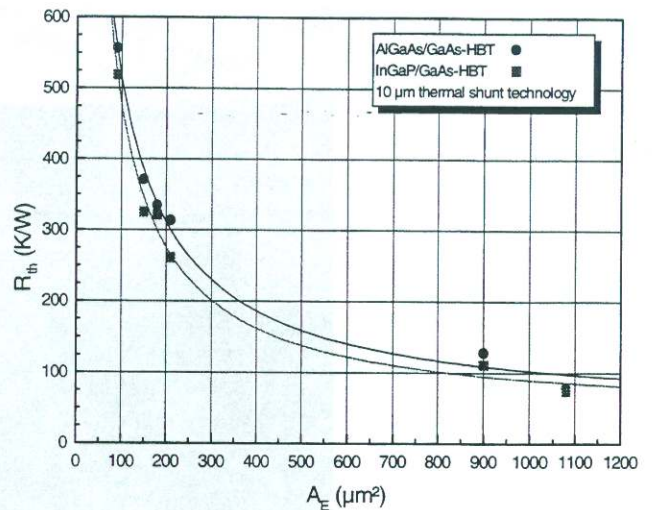


Fig. 4 Measured thermal resistance R_{th} versus emitter area A_E

Power measurements were carried out on the wafer at 2 GHz using an active load-pull system for large signal characterization. The input load reflection coefficient is adjusted to reach maximum output power. Fig. 5-a shows the output power P_{out} and power added efficiency PAE against input power P_{in} , measured at V_{CE} of 3 V for a power cell of $12 \times 30 \mu\text{m}^2$ emitter area. The device delivered an output power of 1 W corresponding to a power density of 2.8 W/mm^2 with more than 56 % PAE. These data demonstrate, that the developed HBTs have a great potential for wireless mobile PCN applications.

Fig. 5-b shows the dependence of P_{out} and PAE on the operating voltage V_{CE} . As the collector-emitter voltage increases both output power and efficiency increase. The power cell HBTs reach peak performance at 8 V with 3 W output power (power density of 8.4 W/mm^2) and more than 70 % power added efficiency. These results show high power handling capabilities of HBTs also under high bias operations.

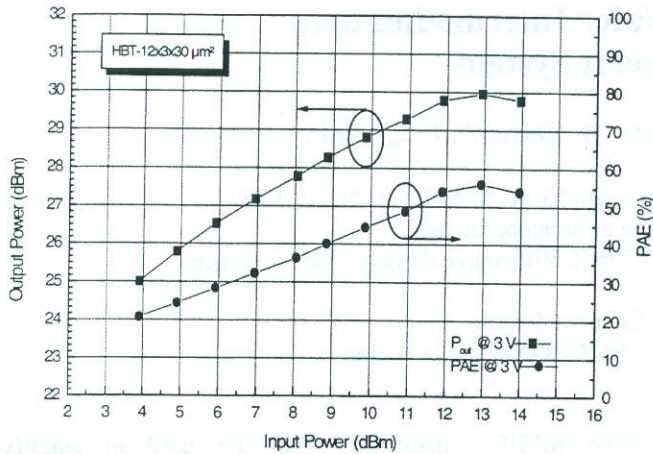


Fig. 5-a Output power P_{out} and power added efficiency PAE against input power P_{in} , measured at 2 GHz for a $12 \times 3 \times 30 \mu\text{m}^2$ HBT ($V_{CE}=3 \text{ V}$)

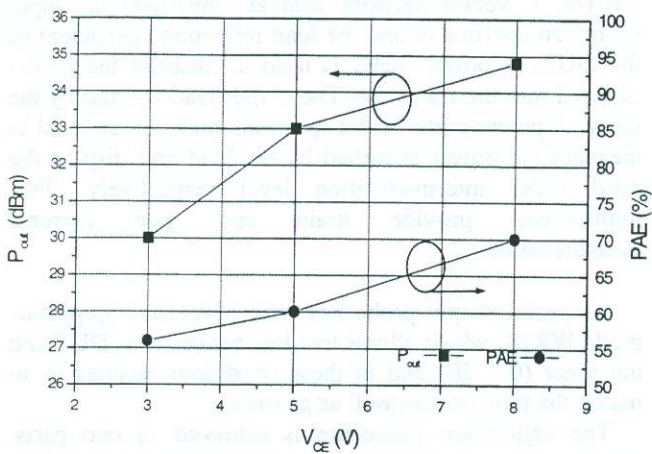


Fig. 5-b P_{out} and power added efficiency PAE against operating bias V_{CE} , measured at 2 GHz for a $12 \times 3 \times 30 \mu\text{m}^2$ power HBT

Fig. 6 shows first results of reliability test performed on a $3 \times 30 \mu\text{m}^2$ InGaP HBT at room temperature under a high collector current density of $1 \times 10^5 \text{ A/cm}^2$ and a collector-emitter voltage of 3 V during 1500 h. After the initial reduction of the current gain by 20 %, the power HBT shows a stable operation for more than 1500 h despite of the high current density used. The current gain degradation is around 4 % for 1500 h stress time and the HBT junction temperature is $165 \text{ }^\circ\text{C}$. These results show the capability of InGaP based HBTs for stable operation at high current level as needed for microwave power amplifiers.

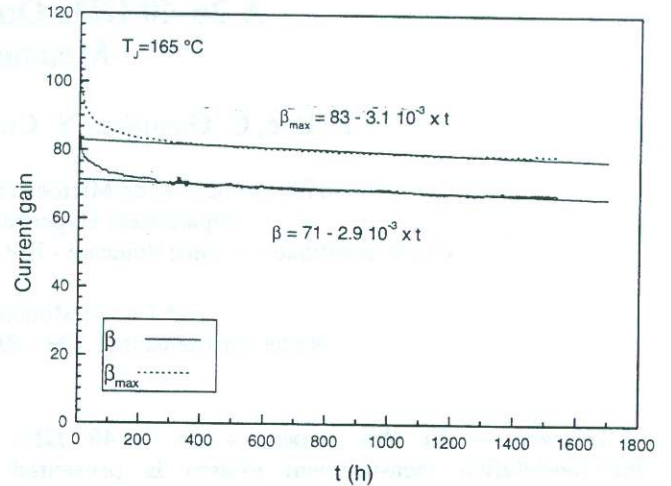


Fig. 6 Life time measurement of a $3 \times 30 \mu\text{m}^2$ HBT at $J_{CE}=1 \times 10^5 \text{ A/cm}^2$ and $V_{CE}=3 \text{ V}$

IV. CONCLUSION

We have developed high performance AlGaAs(InGaP)/GaAs HBTs for use in mobile communications. The device layout is optimized for high microwave performance and low thermal resistance while maintaining a compact chip sizes. The developed power HBTs with $12 \times 3 \times 30 \mu\text{m}^2$ emitter area exhibit 1 W output power and 56 % power added efficiency at 3 V operating bias and 2 GHz. Compared to available power amplifiers for wireless applications, our HBTs have a superior power density of 2.8 W/mm at 3V.

ACKNOWLEDGMENT

The authors would like to thank the German Federal Ministry for Education and Science for financial support (BMBF contract No. 01BM608), and Infineon Technologies AG and United Monolithic Semiconductors GmbH for close collaboration.

V. REFERENCES

- [1] M Achouche, S Hähle, P Heymann, W John, S Kraus, M Mai, D Rentner, E Richter, T Spitzbart, P Wolter, H Wittrich, J Würfl, G Tränkle, „AlGaAs/GaAs heterojunction bipolar transistors for L-band applications“, in 22nd WOCSDICE, pp. 47-48, May 1998
- [2] N. Bovolon, P. Baureis, J.-E. Müller, P. Zwicknagl, R. Schultheis, E. Zanoni, „A simple method for the thermal resistance measurement of AlGaAs/GaAs HBTs“, IEEE Transactions on Electron Devices, Vol. 45, No. 8, pp. 1846-1848, Aug. 1998